Journal of Materials Chemistry A

Solvent mixtures for improved electron transfer kinetics of titanium-doped polyoxovanadate-alkoxide clusters

Journal:	*Journal of Materials Chemistry A*
Manuscript ID	TA-ART-02-2023-001179.R1
Article Type:	Paper
Date Submitted by the Author:	12-Apr-2023
Complete List of Authors:	Dagar, Mamta; University of Rochester, Chemistry Corr, Molly; University of Rochester, Chemistry Cook, Timothy; University at Buffalo, Chemistry McKone, James; University of Pittsburgh, Chemical and Petroleum Engineering Matson, Ellen; University of Rochester, Chemistry

ARTICLE

Solvent mixtures for improved electron transfer kinetics of titanium-doped polyoxovanadate-alkoxide clusters

Received 00th January 20xx,
Accepted 00th January 20xx

DOI: 10.1039/x0xx00000x

Mamta Dagar,[a] Molly Corr,[a] Timothy R. Cook,[b] James R. McKone,*[c] and Ellen M. Matson*[a]

Emergent, flowable electrochemical energy storage technologies suitable for grid-scale applications are often limited by sluggish electron transfer kinetics that impede overall energy conversion efficiencies. To improve our understanding of these kinetic limitations in heterometallic charge carriers, we study the role of solvent in influencing the rates of heterogeneous electron transfer, demonstrating its impact on the kinetics of di-titanium substituted polyoxovanadate-alkoxide cluster, $[Ti_2V_4O_5(OMe)_{14}]$. Our studies also illustrate that the one electron reduction and oxidation processes exhibit characteristically different rates, suggesting that different mechanisms of electron transfer are operative. We report that a 1:4 v/v mixture of propylene carbonate and acetonitrile can lead to a three-fold increase in the rate of electron transfer for one electron oxidation, and a two-fold increase in the one electron reduction process as compared to pure acetonitrile. We attribute this behavior to solvent – solvent interactions that lead to a deviation from ideal solution behavior. Coulombic efficiencies ≥ 90% are maintained in MeCN – PC mixtures over 20 charge/discharge cycles, greater than the efficiencies that are obtained for individual solvents. The results provide insight into the role of solvent in improving the rate of charge transfer and paves a way to systematically tune solvent composition to yield faster electron transfer kinetics.

Introduction

Redox-flow batteries (RFBs) constitute an emerging battery technology, in which electrochemical energy is stored in the form of flowable, redox-active molecules.[1] This design feature gives RFBs advantages over other energy storage systems when used for grid-scale energy storage, including longer active species lifetimes and decoupled power (energy per unit time) and energy (storage capacity).[1-4] However, low energy and power densities and inefficiency of RFB technologies have impeded their widespread application to date.[4-6]

In RFBs, the redox reactions of the electroactive couple at the electrode-electrolyte interface define important characteristics related to battery operation. In particular, the rates of diffusion (as reflected in the diffusion coefficient of the active species, D_0) and electron transfer between charge carrier and electrode surface (as reflected by the heterogeneous electron transfer rate constant, k_0) have emerged as important elements for improving the voltage efficiency of a battery,[7-10] The voltage efficiency of RFBs is influenced by three major parameters: (1) transport losses that occur due to physical characteristics like diffusivity, viscosity, and solubility of the active species;[11] (2) resistive losses that arise from the architecture of the electrodes and current collectors as well as the electrolyte composition;[12] and (3) kinetic losses that result from sluggish electron transfer kinetics. These kinetic limitations predominantly manifest in (dis)charging overpotentials necessary to generate an appreciable current density (≥ tens of mA/cm^2) in a RFB.[13] As such, electron transfer plays a significant role in determining the maximum power density that can be achieved in an RFB, while maintaining a target voltage efficiency.

Given this design criteria, a popular method of RFB electrolyte development is the design of organic or organometallic molecules hypothesized to exhibit intrinsically fast, outer-sphere electron transfer reactions. Indeed, the use of metal-derived coordination complexes in non-aqueous RFBs has received special attention, as binding of ligands to a simple metal salt can dramatically change the solubility and reduction potentials (i.e. cell voltage, V_{cell}) of the redox active ion in organic solvent.[14-20] Several studies have focused on the viability of monometallic complexes as charge carriers for RFBs; however, these complexes often suffer from redox instability and sluggish electron transfer kinetics.[21, 22] To circumvent these challenges, our group[23-25] and others[26-30] have explored the use of multimetallic systems, leveraging electron transfer reactions that result in (de)population of delocalized molecular orbitals. This strategy limits kinetically costly structural perturbations that occur upon oxidation/reduction.

To this end, our team has described polyoxovanadate-alkoxide (POV-alkoxide) clusters as an alternative class of charge carriers for symmetric non-aqueous RFBs (**Figure 1**). Our research team has demonstrated that incorporating bridging alkoxide ligands at the surface of the redox-active vanadium

[a] Department of Chemistry, University of Rochester, Rochester NY 14627, USA.
[b] Department of Chemistry, University at Buffalo, The State University of New York, Buffalo NY 14260, USA.
[c] Department of Chemical and Petroleum Engineering, University of Pittsburgh, Pittsburgh PA 15261, USA.

Electronic Supplementary Information (ESI) available: Experimental procedures, spectroscopic and analytical data. For ESI or other electronic format see DOI: 10.1039/x0xx00000x

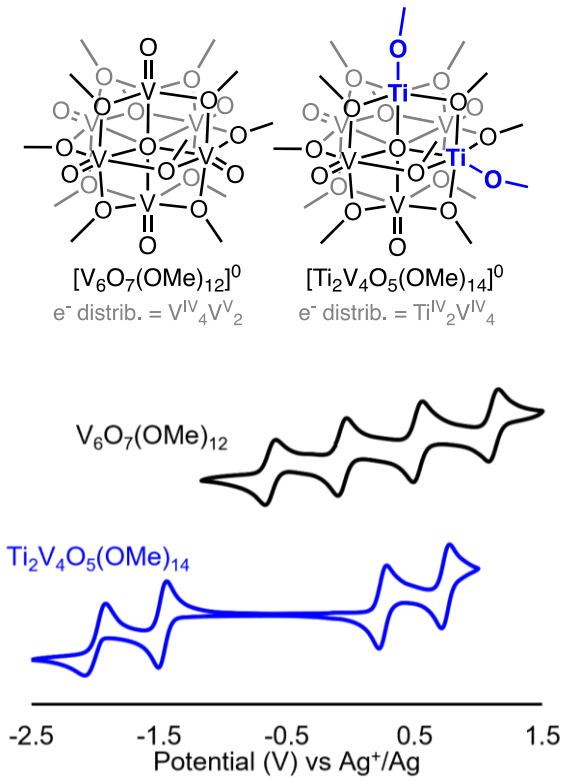

Figure 1. POV-alkoxide clusters as charge carriers for non-aqueous RFBs (top); cyclic voltammograms of $V_6O_7(OMe)_{12}$ (black) and $Ti_2V_4(OMe)_{14}$ (blue; bottom).

oxide assembly improves the solubility of the cluster in organic solvent, and enhances the stability of the mixed-valent, Lindqvist core across multiple charge states.[23-25, 31, 32] Notably, the availability of five redox states in a single molecule also enables operation of the resultant non-aqueous RFB in a symmetric configuration, where the negative and positive electrolytes use same POV-alkoxide cluster as the redox-active species. This drastically reduces the negative impact of chemical contamination associated with electrolyte crossover. Moreover, heterometal incorporation has proved to effectively increase the V_{cell} of the system, while retaining the characteristic electrochemical reversibility and stability of the homometallic POV-alkoxide.[33] Most relevant to this work, these clusters exhibit excellent electrokinetic properties in acetonitrile. These attributes prompt additional investigations to further understand and improve the electrochemical behaviour of these species in non-aqueous media.

Herein we report the effect of modifying solvent composition on diffusion and electron transfer for the heterometallic POV-alkoxide cluster, $[Ti_2V_4O_5(OMe)_{14}]$ (**Figure 1**). We demonstrate that the solvent effect is manifold, arising from both alterations in the chemical nature of the solvent and charge carrier - solvent interactions in the transition state. We also assess the ability of solvent mixtures to further improve the rate of electron transfer. These results highlight the importance of considering solvent-solvent interactions while choosing binary solvent mixtures for designing robust redox systems.

While the effect of mixed solvents on the performance of RFBs has been explored previously,[34-36] this work expands upon these ideas through the discussion of transport and kinetic losses that influence the voltage efficiency of an RFB. For instance, Li and co-workers report that organic charge carriers in a non-aqueous RFB exhibit varied diffusivity upon addition of co-solvent.[34] The authors predict that depressions in diffusivity lead to slower electrode kinetics, suggesting solvent choice is important in the construction of a flow cell. However, experimental measurements were not made to correlate diffusion coefficients and electron transfer rate constants. In our experiments, we observe that slower diffusivity does not always translate into slower rates of electron transfer.

In other work, the effect of binary and ternary solvent mixtures on symmetric non-aqueous RFBs composed of vanadium acetylacetonate charge carriers has been studied.[35, 36] Both studies focus on distinct behaviours of assessing battery performance rather than a comprehensive analysis of the system. For example, Herr et al. study electron transfer kinetics in only the solvent system that exhibits maximum solubility. Almheiri and co-workers limit their work to developing an understanding of the rates of electron transfer at the electrode surface. Both of these studies use narrow scan rate windows (10 – 100 mV/s) to determine the kinetics of charge carriers. It has been demonstrated that a reliable k_0 value employs a wider range of scan rates.[37, 38] In our work, we present a detailed analysis of the electron transfer kinetics, battery charge-discharge data and diffusivity in binary solvent mixtures. Moreover, we employ a scan rate range of 10 – 10000 mV/s to get an estimate of the upper bound of the heterogeneous rates of electron transfer. Importantly, our findings present an improved understanding of factors that influence power-densities in non-aqueous RFBs.

Experimental

General considerations. All manipulations were carried out in the absence of water and oxygen in a UniLab MBraun inert atmosphere glovebox under a dinitrogen atmosphere. Glassware was oven dried for a minimum of 4 hours and cooled in an evacuated antechamber prior to use. Anhydrous propylene carbonate, dimethylformamide, and dimethylsulfoxide were purchased from Sigma-Aldrich and stored over activated 4 Å molecular sieves purchased from Fisher Scientific. All other solvents were dried and deoxygenated on a Glass Contour System (Pure Process Technology, LLC) and stored over activated 3 Å molecular sieves purchased from Fisher Scientific. Tetrabutylammonium hexafluorophosphate ($[^nBu_4N][PF_6]$) was purchased from Sigma-Aldrich, recrystallized thrice using hot methanol, and stored under dynamic vacuum for a minimum of two days prior to use. $[Ti_2V_4O_5(OMe)_{14}]$ was synthesized according to literature precedent.[25]

Cyclic voltammetry. Cyclic voltammetry (CV) was performed using a three-electrode setup inside a nitrogen filled glove box (MBraun UniLab, USA) using a Bio-Logic SP 150 potentiostat/galvanostat and the EC-Lab software suite. The concentration of $[Ti_2V_4O_5(OMe)_{14}]$ and $[^nBu_4N][PF_6]$ were kept at 5 mM and 100 mM, respectively, throughout all

measurements. CVs were recorded using a 3 mm diameter glassy carbon working electrode (CH Instruments, USA), a Pt wire auxiliary electrode (CH Instruments, USA), and a Ag/Ag^+ non-aqueous reference electrode with 0.01 M $AgNO_3$ in 0.1 M $[^nBu_4N][PF_6]$ in MeCN (BASi, USA). CVs were iR compensated at 95% with impedance taken at 100 kHz using the ZIR tool included within the EC-Lab software. The remaining 5% uncompensated resistance was accounted for by manual correction using the strategy described by Myland and Oldham.[39]

***Bulk electrolysis*.** Bulk electrolysis experiments were performed in a H-cell with a glass frit separator (Porosity = 10-16 µm, Pine Research, USA) using a Bio-Logic SP 150 potentiostat/galvanostat. In all experiments, an active species concentration of 5 mM was used. The working electrode compartment contained 10 mL of the active species with 0.1 M $[^nBu_4N][PF_6]$ in the desired solvent, while the counter electrode compartment had 10 mL of 0.1 M $[^nBu_4N][PF_6]$ in the desired solvent. A Pt mesh working electrode and a Pt wire counter electrode were used. Bulk electrolysis experiments were carried out using the chronoamperometry techniques available in EC-Lab software suite at constant potentials, selected from CV.

***Solubility measurements*.** All samples were prepared in the absence of water and oxygen using a Unilab MBraun inert atmosphere glovebox under dinitrogen atmosphere. A 0.1 M concentration of $[^nBu_4N][PF_6]$ was used in all samples to simulate electrochemical conditions. All electronic absorption spectra were measured using an Agilent Cary 60 UV-Vis spectrophotometer. All samples were referenced against a baseline of 0.1 M $[^nBu_4N][PF_6]$ in the corresponding solvent.

To establish a calibration curve for each solvent, 12.5 mM stock solutions were prepared by combining 0.194 g $[^nBu_4N][PF_6]$, 0.051 g $[Ti_2V_4O_5(OMe)_{14}]$, and 5 mL of solvent in a vial and stirring until completely dissolved. 2 mL of this solution were removed and diluted to 20 mL using a 0.1 M solution of $[^nBu_4N][PF_6]$ in solvent. 4 mL of this 1.25 mM solution were transferred to a cuvette, and the volume of the solution was restored. This process was repeated to obtain 5 calibration solutions with the following concentrations: 1.25 mM, 1.00 mM, 0.80 mM, 0.64 mM, and 0.51 mM. After recording the electronic absorption spectra of each sample, absorbances at 424 nm were plotted against the sample's concentration to obtain a Beer's law equation.

Three saturated solutions for each solvent were prepared by stirring an excess of $[Ti_2V_4O_5(OMe)_{14}]$ in 5 mL of 0.1 M $[^nBu_4N][PF_6]$ solution for a minimum of 24 hours. These solutions were passed through a syringe filter (EZFlow Syringe Filter, diameter = 25 mm, pore size = 0.22 µm) to remove undissolved $[Ti_2V_4O_5(OMe)_{14}]$. 25 µL aliquots of each solution were removed and diluted to a known volume with absorbance between 0.1 and 1.0. The absorbance of each diluted sample at 424 nm was recorded, and the concentration of the dilute was calculated using Beer's law equation from the corresponding calibration curve. The original concentration of the saturated solution was then calculated from the concentration of the diluted sample.

***Charge/discharge experiments*.** Charge/discharge testing was conducted in a nitrogen filled glove box using a glass H-cell separated by a microporous glass frit (P5, 1.6 µm, Adams and Chittenden, USA) and a Bio-Logic SP 300 potentiostat/galvanostat. The electrolyte solutions used in charge/discharge experiments were 5 mM $[Ti_2V_4O_5(OMe)_{14}]$ in 0.1 M $[^nBu_4N][PF_6]$ in the given solvent or solvent mixture. Each compartment of the H-cell was filled with 5.0 mL of the electrolyte solution. Two graphite felt electrodes (1 × 1 × 0.5 cm, Fuel Cell Store, USA) were placed in the posolyte and negolyte chambers. Electrodes attached to Pt wire current collectors submerged in the electrolyte solutions (~0.5 cm). Graphite felt electrodes were soaked in electrolyte solutions for 24 hours before each experiment. A sequential galvanostatic – potentiostatic charge/discharge method was adopted using a charging current of 0.2 mA until the potential reached 1.9 V.[40] Subsequently, the potential was held at 1.9 V until the current dropped to 0.02 mA. Similarly, a discharging current of |0.2 mA| was applied until a cut-off potential of 1.4 V was reached, followed by a potentiostatic discharge at 1.4 V until the current reached a value of |0.02 mA|. During all charge/discharge experiments, both half cells were stirred at ~1,000 rpm.

Viscosity measurements. Solution viscosities were measured using a TA Instruments Discovery HR-2 rheometer. A 40 mm parallel-plate geometry and standard Peltier plate were used for the experiments. The gap was maintained at 53 µm was used for all measurements. Eight shear rates per decade from 1 – 100 s^{-1} were sampled. The average dynamic viscosity reported was calculated from shear rates of 10 s^{-1} and higher.

Results and Discussion

Despite the fact that the electrochemistry of RFB electrolytes can be heavily impacted by the solvent medium, little progress has been made in elucidating the underlying factors responsible for the variations in redox reactivity that are observed as solvent is altered.[35, 36, 41] Acetonitrile is the most popular solvent for non-aqueous RFB chemistry due to several key properties. The first is low viscosity, which enhances diffusivity of electroactive species from bulk solution to the electrode-electrolyte interface. Furthermore, this solvent exhibits

Table 1. Properties of solvents studied in this work at room temperature (25 °C).

Solvent	Dielectric constant[42]	Viscosity[43] cP	Donor number[44]	Acceptor number[44]	$E_T(30)$[45] Kcal/mol	Density g/mL
MeCN	36.64	0.369	14.1	18.9	45.6	0.786
DMSO	47.24	1.987	29.8	19.3	45.1	1.100
DMF	38.25	0.794	26.6	16.0	43.8	0.944
PC	64.92	2.53	15.1	18.3	46.0	1.204
DCM	8.93	0.413	1.0	20.4	41.1	1.386

Scheme 1. Relevant electrochemical processes for $[Ti_2V_4O_5(OMe)_{14}]$.

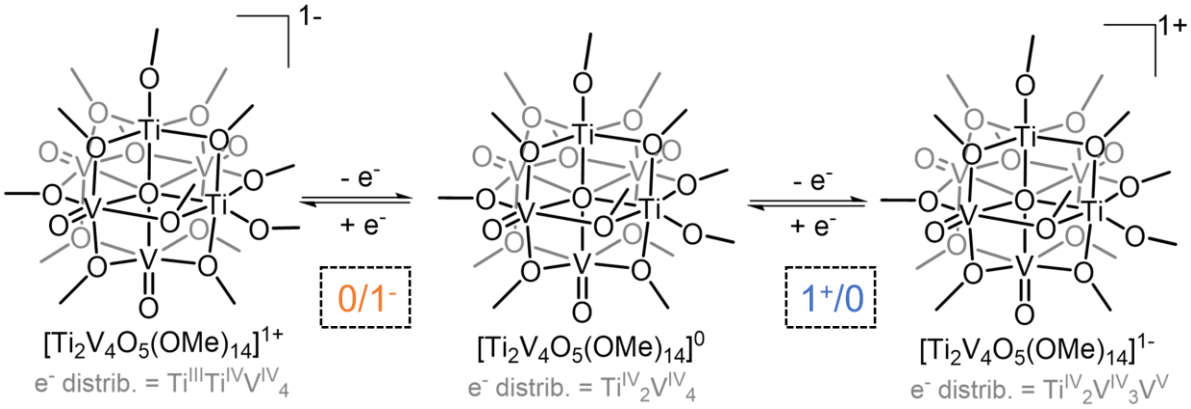

excellent electrochemical stability at extreme operating potentials and a high dielectric constant; the latter property leads to higher conductivity upon dissolution of supporting electrolyte.[14] However, acetonitrile is also expensive, flammable, and volatile.[15] These issues necessitate identification of other suitable organic solvents for non-aqueous RFBs.

As such, we set out to develop an improved understanding of the electrochemical properties of $[Ti_2V_4O_5(OMe)_{14}]$ at glassy carbon electrodes in a variety of organic solvents, namely acetonitrile (MeCN), propylene carbonate (PC), dichloromethane (DCM), dimethylformamide (DMF), and dimethylsulfoxide (DMSO). Solvent selection was motivated by literature precedent;[35, 36, 41] each solvent offers a large window of electrochemical stability while differing substantially in key physicochemical properties like dielectric constant[42], viscosity[43], donor number[44], and acceptor number[44], $E_T(30)$[45] (**Table 1**). This, in turn, enables connections to be made between the properties of these solvents, electron-transfer kinetics, and solubility of the POV-alkoxide cluster.

We opted to study the heterometal substituted assembly, $[Ti_2V_4O_5(OMe)_{14}]$, due to prior work describing key properties of solubility, stability, and electrochemical reactivity that make this type of assembly promising for use as a charge carrier in a symmetric RFB.[33] Electrochemical analysis of $[Ti_2V_4O_5(OMe)_{14}]$ reveals a set of four redox events in the potential range from -2.5 V to +1.0 V vs. $Ag^{+/0}$ in MeCN (**Figure 1**). The oxidation events are attributed to the successive, one-electron vanadium-based processes ($V^{IV} \rightarrow V^{V} + e^-$), while the two sequential reductions have been assigned to the reduction of the two titanium ions in the Lindqvist core ($Ti^{IV} + e^- \rightarrow Ti^{III}$). The di-cationic and di-anionic derivatives of $[Ti_2V_4O_5(OMe)_{14}]$ are prone to decomposition in all solvents analysed; hence, we limit our studies to the quasi-reversible one electron reduction (**0/1**$^-$) and oxidation (**1**$^+$**/0**) processes of the neutral cluster (**Scheme 1**). As shown in **Figure 1**, these redox events are separated by a V_{cell} of 1.73 V.

The reported solubility of $[Ti_2V_4O_5(OMe)_{14}]$ in MeCN is 0.193 M, resulting in a theoretical energy density of ~ 4.44 Wh L^{-1}. This theoretical energy density is somewhat lower than previously reported metal-derived charge carriers for non-aqueous RFBs, such as $[Ru(bpy)_3]^{2+}$ (6.94 Wh L^{-1})[14] and $[Cr(L)_3]$ (7.22 Wh L^{-1}, where ligand L = 4,4'-(bis(2-(2-methoxyethoxy)-ethyl)ester)-2,2'-bipyridine)[46]. However, prior reports from our group have demonstrated that surface ligand modification of POV-alkoxides can result in solubilities as high as ~1 M.[23, 24, 31] Surface functionalization of these titanium-doped POV-alkoxide clusters is the subject of ongoing efforts in our laboratory.

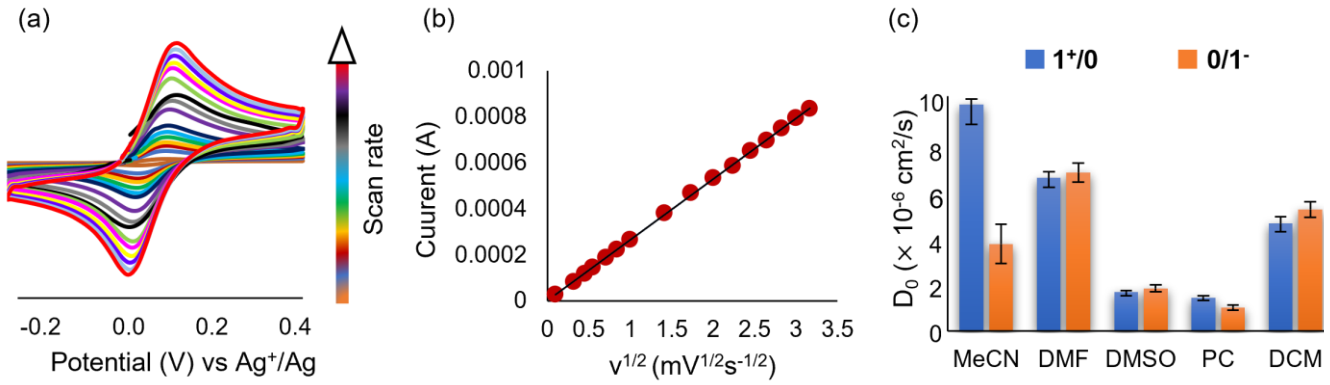

Figure 2. (a) Representative CV measurements of **1**$^+$**/0** redox couple of 5 mM $[Ti_2V_4O_5(OMe)_{14}]$ with 0.1 M $[^nBu_4N][PF_6]$ in MeCN at scan rates ranging from 10 – 10000 mV/s; (b) Randles – Sevcik analysis of the corresponding data in MeCN; (c) Diffusion coefficients in studied solvents. **1**$^+$**/0** denotes one-electron oxidation, and **0/1**$^-$ denotes one-electron reduction of the neutral cluster. The method used to calculate error is included in the Supporting Information.

Solvent effect on Transport properties – Diffusivity, Viscosity, and Conductivity measurements

A key requirement of an efficient RFB is the rapid diffusivity of the charge carriers (including the redox couple and the supporting electrolyte species) in the electrolyte.[47] To determine the diffusion coefficients for $[Ti_2V_4O_5(OMe)_{14}]$ across different solvents, the redox events associated with **1⁺/0** and **0/1⁻** were isolated and CVs were recorded at scan rates ranging from 10 – 10,000 mV/s (**Figure 2,** Figures S1-S5 and S7-S11). In all solvent systems, the plot of the peak current (i_p) versus the square root of scan rate ($v^{1/2}$) exhibits a linear dependence (**Figure 2a-2b**, Figures S6 and S12). This behaviour is characteristic of a diffusion-limited electrochemical process, allowing for the assessment of the D_0 of $[Ti_2V_4O_5(OMe)_{14}]$ in each solvent using the Randles-Sevcik (R-S) equation (**Figure 2c**).[48, 49]The calculated D_0 values for **1⁺/0** and **0/1⁻** of $[Ti_2V_4O_5(OMe)_{14}]$ range from 10^{-6} to 10^{-5} cm^2 s^{-1} in all solvents evaluated. These values are similar to those reported previously for molecular RFB charge carriers,[47, 50, 51] including small organic compounds (e.g. tris(dialkylamino)cyclopropenium ions, 7.0 × 10^{-6} cm^2 s^{-1};[52] quinone, 1.13 × 10^{-5} cm^2 s^{-1}).[53] This observation is surprising, given the high molar mass of the POV-alkoxide cluster (813.97 g mol^{-1}). We note, however, the cross-sectional area of $[Ti_2V_4O_5(OMe)_{14}]$ (73.8 Å²) is similar to that of quinones (21.2 Å² (unsubstituted) – 128.6 Å² (substituted), as estimated using crystallographic data, justifying the comparable measured values of D_0.[54, 55]

D_0 of $[Ti_2V_4O_5(OMe)_{14}]$ is significantly higher in MeCN, DMF, and DCM (~7 ×10^{-6} cm^2/s) as compared to PC and DMSO (~2 × 10^{-6} cm^2/s). The observed difference in these values of diffusivity across this series of solvents translates into a proportional difference in the maximum current density that can be achieved in a mass-transfer limited regime under RFB operation. We rationalize the varied D_0 values using relative solvent viscosities. As can be seen from Table 1, MeCN has the lowest viscosity, translating to the most rapid diffusion of $[Ti_2V_4O_5(OMe)_{14}]$ in solution. While DMF has higher dynamic viscosity than DCM at room temperature, its density is appreciably lower than that of DCM. As a result of this trade off, diffusion of $[Ti_2V_4O_5(OMe)_{14}]$ in DMF is more rapid (larger value of D_0) than that measured for the heterometallic POV-alkoxide cluster in DCM. Both DMSO and PC have an appreciably high solvent viscosity; unsurprisingly, $[Ti_2V_4O_5(OMe)_{14}]$ diffuses more slowly in these solvents.

Solvent effect on electrokinetic parameters (k_0)

Solvent identity influences the kinetics of electron transfer at the electrode surface in many ways. For example, modification of solvent system significantly changes the composition and structure of the double layer due to the dielectric properties of the surrounding medium. This results in changes in Gibbs free energy of activation for electron transfer reactions due to differences in solvation of the activated complex at the electrode surface.[56] The solvent system also plays a significant role in dictating the pre-exponential factor of the electron-transfer rate constant, as the dynamic properties of the solvent influences the frequency of the formation of the activated complex and the frequency with which it decays to form the product.[44, 57, 58]

Given this information, we became interested in investigating the way in which electron transfer rate constants change as a function of solvent composition. Experimental heterogeneous electron transfer rate constants (k_0) for **1⁺/0** and **0/1⁻** in each solvent were estimated using the Nicholson method (Figures S14-S17).[59] This method uses variable scan rate CV data to estimate k_0 by correlating the difference in peak potential (ΔE_p) with a dimensionless kinetic parameter (Ψ). Ψ was obtained by using an empirical fit to Nicholson's original data in the range from $0.1 < \Psi < 20$ given in eq. 1:[60]

$$\Delta E_p \cdot n = 0.054 + 0.03103\Psi^{-0.7078} \qquad (1)$$

Nicholson demonstrated that for quasi-reversible electron-transfer, Ψ can be related to k_0 by using eq. 2:

$$\Psi = \nu^{-\frac{1}{2}} k_0 \left(\pi n F D_0 / RT\right)^{-\frac{1}{2}} \qquad (2)$$

where n is the number of electrons involved in the reaction, ν is the scan rate, F is the Faraday constant, Ψ is Nicholson's dimensionless parameter, D_0 is the diffusion coefficient, R is the gas constant, and T is temperature. A plot of Ψ vs $v^{-1/2}$ should give a line with y-intercept of zero and a slope that is proportional to k_0. The calculated values of k_0 for **1⁺/0** and **0/1⁻**

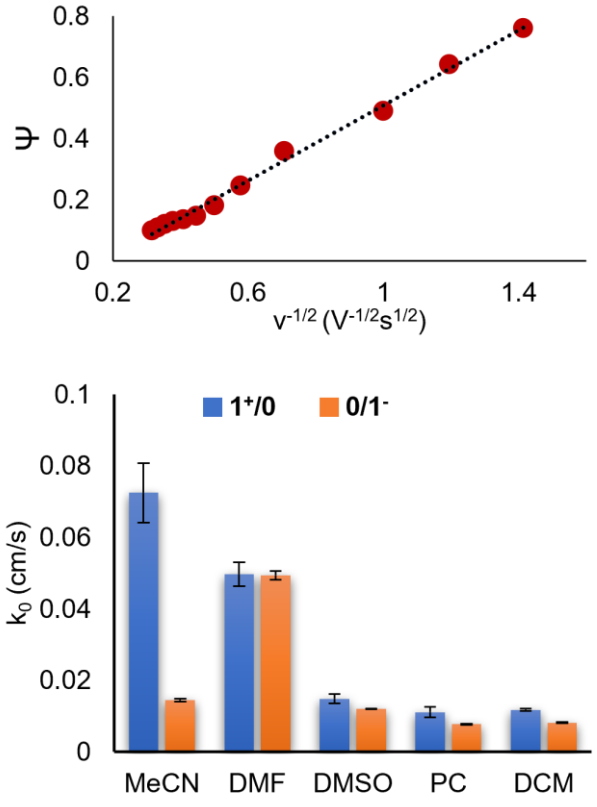

Figure 3. Representative Nicholson fit of the **0/1⁻** redox couple in MeCN (top); Heterogeneous electron transfer rate constants for one-electron oxidation (**1⁺/0**) and reduction (**0/1⁻**) in different solvents (bottom). Error bars (shown in black) indicate the standard error associated with each data set in the 95% confidence interval of the regression analysis.

of $[Ti_2V_4O_5(OMe)_{14}]$ are plotted in **Figure 3.** It should be noted that the rate constants of electron transfer for **1⁺/0** and **0/1⁻** in MeCN are larger than the previously reported values from our group (**1⁺/0** = 2.3 × 10^{-2} cm/s; **0/1⁻** = 3.6 × 10^{-3} cm/s).[33] This is due to the fact that in the present work the range of scan rates (10 – 10,000 mV/s) used is greater than that of the prior study (10 – 1000 mV/s), which gives a more accurate measure of the kinetics in this range of k_0 values.

For **1⁺/0**, the fastest electron transfer rate constant is observed in MeCN, whereas DMF offers the highest rate of electron transfer for **0/1⁻** (**Figure 3**). Notably, electron transfer rate constants are comparable for both the redox events in all the solvents except MeCN. In MeCN, reduction of the neutral cluster is significantly inhibited, rendering k_0 of **0/1⁻** comparable to values found in more viscous solvents (e.g., DMSO, PC). In an attempt to explain the differences observed in the apparent rate of electron transfer, we evaluated additional solvent properties (e.g. dielectric relaxation time and solvent polarity parameter) and their correlation to k_0. Interestingly, k_0 values for **0/1⁻** are inversely proportional to the acceptor number (AN) of the solvent (**Figure 4**), in that the apparent rate constant decreases with increase in solvent acidity. This finding suggests that the AN of a solvent correlates to its ability to stabilize the reduced form of the cluster; as the acidity of the solvent increases, its ability to solvate anions and Lewis bases increases.[61] This leads to an increased stabilization of the reduced product and the transition state at the expense of destabilizing the neutral cluster. The change in differential stabilization increases the activation energy of the electron transfer process, thereby decreasing k_0.

In contrast, comparison of k_0 values for **1⁺/0** to solvent AN reveals no correlation (Figure S18). This result is unsurprising, as a more acidic solvent is not expected to readily stabilize the positive charge of the cluster following oxidation. However, we also found no correlation between k_0 and donor number (DN) or any of the other solvent properties we tabulated (e.g., dielectric relaxation time, optical or static dielectric constant, polarizability, hydrogen bond acidity/basicity).

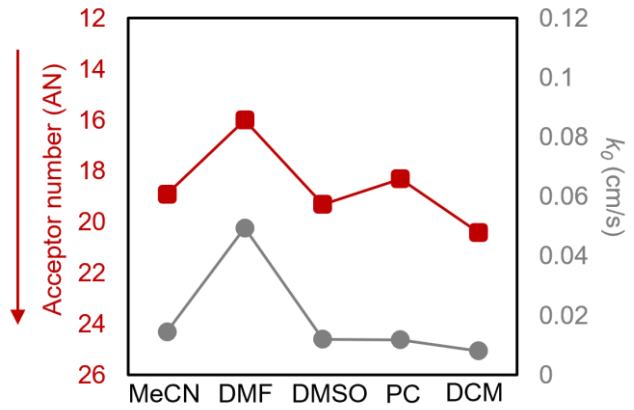

Figure 4. Comparison between acceptor number (AN) of the solvent and apparent rate of electron transfer (k_0) for the reduction process.

Mixed solvent systems

Our initial studies demonstrated how the transport properties and electron transfer kinetics of $[Ti_2V_4O_5(OMe)_{14}]$ change as a function of solvent. While DMF proved to be a reasonable solvent based on these characteristics, the oxidative instability of $[Ti_2V_4O_5(OMe)_{14}]$ renders it incompatible for battery cycling (Figure S23). DCM offers slower rates of electron transfer despite exhibiting high diffusivity. Furthermore, this solvent is volatile, increasing the health risks associated with its use and challenges with technological implementation. Based on these observations, we conclude that MeCN and PC are the only viable solvents of those evaluated for potential use in non-aqueous RFBs based on $[Ti_2V_4O_5(OMe)_{14}]$.

PC is an important solvent used in lithium-ion battery (LIB) electrolytes due to its high dielectric constant, low melting point, wide electrochemical window, and good compatibility with various transition metal oxide cathode materials.[62-64] However, its high viscosity reduces the rate of mass transfer when it is used in battery elecrolytes.[65] Previous studies have circumvented this challenge by using PC as an *additive* to existing electrolyte systems for LIBs, resulting in improved

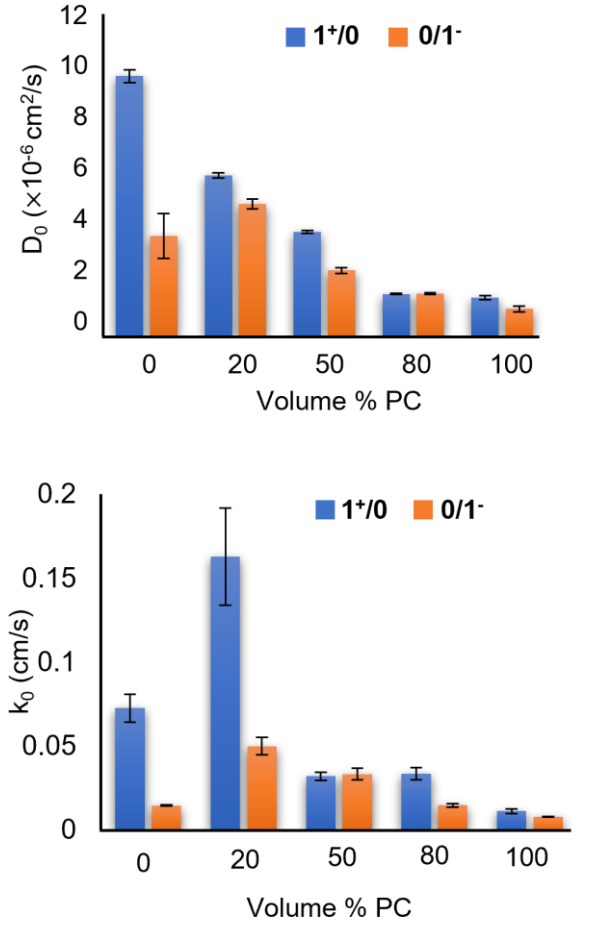

Figure 5. Diffusivity of the heterometallic assembly in MeCN – PC mixtures. (top); Heterogeneous rate constants of electron transfer in MeCN – PC mixtures (bottom). Labels on the x-axis correspond to solvent composition, with pure solvents as end members and ratios listed as percentage of PC.

battery capacity.[66, 67] Hence, we became interested in examining the role of PC as an additive. Toward this goal, we investigated binary mixtures of PC and MeCN with $[Ti_2V_4O_5(OMe)_{14}]$. This, we reasoned, would enable an understanding of the value of mixing solvents which possess extremely different physical properties.

In analogy to the studies described above for single solvent systems, we initially evaluated mass transport properties (e.g., diffusion of charge carrier, viscosity, conductivity) of the POV-alkoxide cluster in mixed solvents. As expected, the diffusivity of $[Ti_2V_4O_5(OMe)_{14}]$ decreases with addition of viscous PC to MeCN (**Figure 5**).

Next, we evaluated the kinetics of electron transfer of the reduction and oxidation of $[Ti_2V_4O_5(OMe)_{14}]$ in these solvent mixtures (**Figure 5**). Interestingly, we observe that with the addition of 20% PC to the MeCN based electrolyte, there is a two-fold increase in the k_0 for the **1$^+$/0** redox couple and a three-fold increase in k_0 for the **0/1$^-$** couple. Furthermore, a 1:1 mixture of MeCN: PC results in similar rates of electron transfer for both the **1$^+$/0** and **0/1$^-$** redox events where both are still markedly faster than the **0/1$^-$** couple in MeCN alone. These results are quite significant, given that higher rate constants are cited to translate to smaller overpotentials and higher efficiencies for operating RFB devices.

To better understand the reason for the distinctive kinetic behaviour in solvent mixtures, we turned to investigations of the thermodynamic consequences of solvent mixing. In liquids, ideality refers to the ability of two or more solvents to retain their individual physicochemical properties when mixed to form a single solution.[68] In other words, solvents A and B behave ideally when they have highly similar intermolecular interactions between A-A, B-B, and A-B. Hence, an ideal mixture of two miscible liquids should follow the mole additive rules for thermodynamic properties like viscosity, as shown in eq. 3:[69]

$$\eta_m^{ideal} = \chi_1 \eta_1 + \chi_2 \eta_2 \qquad (3)$$

where η_1 and η_2 are the molar viscosities of solvents 1 and 2, and χ_1 and χ_2 are their respective mole fractions.

However, real solutions deviate from ideality. **Figure 6** shows that there is a negative deviation from molar additivity over the studied range of compositions. Furthermore, theoretical calculations performed using the Jouyban – Acree model[70] of dynamic viscosity (Eqn 4) also predicts a negative deviation from ideality at the studied concentrations, in agreement with the experimental results.

$$\ln(\eta_{m,T}) = \chi_1 \ln(\eta_{1,T}) + \chi_2 \ln(\eta_{2,T}) + \frac{\chi_1\chi_2}{T}[-61.784 + 54.566(E_{m1} - E_{m2})^2 - 129.759(S_1 - S_2)^2 - 1978.988(A_1 - A_2)^2 + 331.691(B_1 - B_2)^2 + 190.370(V_1 - V_2)^2] + \frac{\chi_1\chi_2(\chi_1 - \chi_2)}{T}[-706.352(A_1 - A_2)^2 + 65.119(V_1 - V_2)^2] \qquad (4)$$

where $\eta_{m,T}$, $\eta_{1,T}$ and $\eta_{2,T}$ are viscosity of mixed solvents and pure solvents 1 and 2 at temperature T, χ_1 and χ_2 are the fractions of the solvents 1 and 2, E_m i s the excess molar refraction, S is polarizability of the analyte, A denotes the analyte's hydrogen-bond acidity, B stands for the analyte's hydrogen-bond basicity and V is the McGowan volume of the analytes.[70] The constants E_m, S, A, B, and V are known as the Abraham solvation parameters.[71] They account for the possible interactions between solvents in a binary mixture and can be used to predict the viscosity of different binary mixtures at various temperatures by employing the corresponding experimental η_1 and η_2 values of the mono-solvents at T.

Our observations in mixed solvents systems suggest that there is a deviation in the viscosity values as would be expected from a linear combination of the two individual solvents or ideal solution behavior (eq. 3). We observe this deviation in the observed values calculated using the Stokes-Einstein equation (depicted in **Figure 6**) and the experimentally evaluated viscosity values (Figure S51). This non-ideality of the electrolyte reflects the presence of intermolecular interactions, which can change as a function of solvent composition. Viscosity is one of the fundamental solvent properties that influences its ability to solvate a molecule,[72] and these same solvation dynamics have a marked impact on electron-transfer rates.[73, 74] Our findings suggest that there is considerable value in further studies that can probe the effect of solvent mixtures with varying degrees of non-ideality on the electrode kinetics of non-aqueous charge carriers.

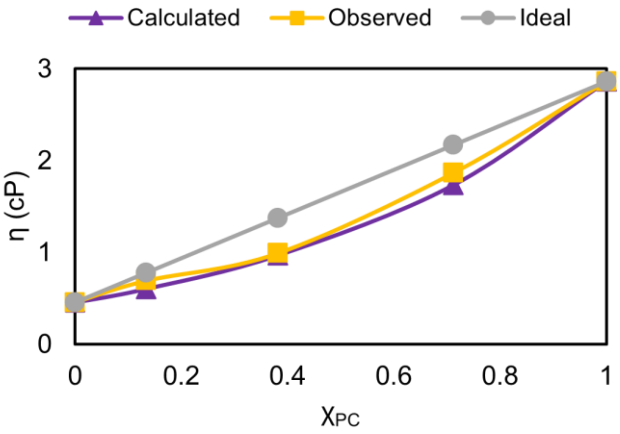

Figure 6. Comparison between the observed values of viscosity, ideal viscosity, and calculated viscosity (using Jouyban-Acree model) in MeCN – PC mixtures.

Charge/discharge experiments

Thus far, we have established the utility of the heterometallic complex, $[Ti_2V_4O_5(OMe)_{14}]$, as a prospective charge carrier in symmetric setups that can transfer one electron at each electrode. With the estimated values of solubility in the binary solvent mixtures (see supporting information), we can predict the theoretical volumetric energy density using eq 5.[75]

$$E = \frac{n V_{cell} C_{active} F}{2} \qquad (5)$$

where, E is the volumetric energy density, n is the number of electrons, V_{cell} is the cell voltage, C_{active} is the concentration of the charge carrier, and F denotes the Faraday's constant. The

V_{cell} is the average discharge voltage of 1.73 V for these mixed systems, and the solubility ranges from 45 – 20 mM. This yields a theoretical energy density in the range of 3.8 – 1.7 kJ/mol.

The attractive physicochemical properties and fast kinetics of the active species inspired further analyses as non-aqueous RFB charge carriers. Even though the studied titanium-substituted POV-alkoxide cluster does not offer high theoretical energy density in MeCN – PC mixtures, nevertheless, we were interested in learning the influence of rate of electron transfer on the battery cycling behavior. Our motivation in performing the charge-discharge experiments is rooted in analyzing how kinetic inhibitions in electron transfer can impact battery performance metrics rather than the amount of charge that can be stored by the cluster.

We performed static charge/discharge cycling experiments with 5 mM solution of the cluster in MeCN with 0.1 M $[^nBu_4][PF_6]$ supporting electrolyte in an H-cell, separated by a glass frit (**Figure 7**). We adopted a galvanostatic–potentiostatic sequential cycling method.[40] A charging current of 0.2 mA until the potential reached 1.9 V, followed by holding the potential at 1.9 V until the current dropped to 0.02 mA. Similarly, a discharging current of |0.2 mA| was applied until a cut off potential of 1.4 V was reached, with a potentiostatic discharge at 1.4 V until the current reached a value of |0.02 mA|. Figure S46 depicts the first 20 cycles observed during the battery cycling experiment in MeCN. Post cycling analysis by CV (**Figure 7b**) demonstrates the stability of the positive electrolyte under the cycling experiments, however slight decomposition of the negative electrolyte was observed. Notably, no additional plateaus were observed due to this decomposition in the obtained data as illustrated in **Figure 7a** for Cycle 2 and 20. This observation further suggests that the nature of the decomposition is chemical rather than electrochemical.

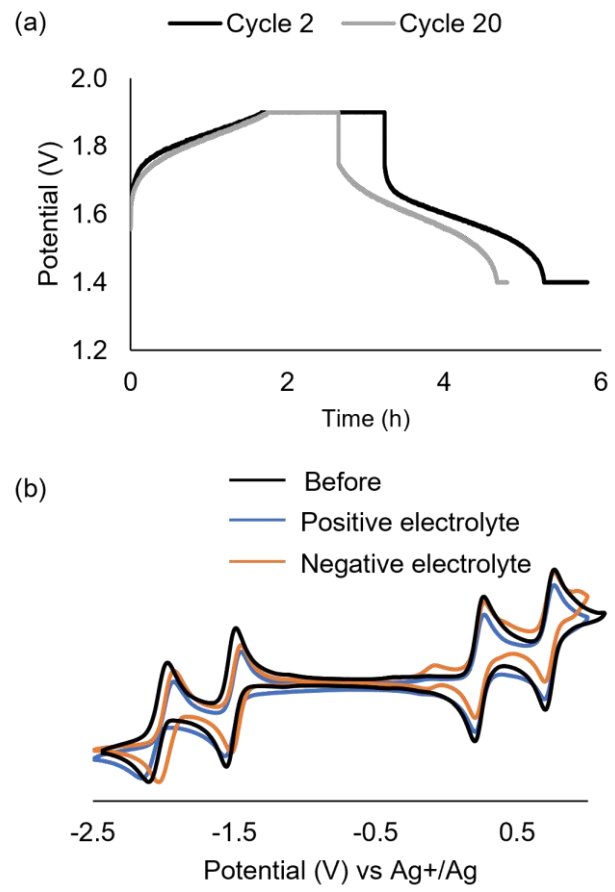

Figure 7. (a) Comparison of cycles 2 and 20 from the battery cycling experiment (b) Cyclic voltammograms of cluster before (black) and after charge-discharge cycles. The orange trace depicts the negative electrolyte whereas the blue trace denotes the positive electrolyte.

The charge-discharge behaviour of $[Ti_2V_4O_5(OMe)_{14}]$ in the present study differs significantly from our prior report in MeCN.[33] We attribute this change to a different battery cycling strategy as well as the choice of the separator. Contrary to the previous work performed under purely galvanostatic charge/discharge conditions, we do not observe any extra plateaus in the battery cycling data as shown in **Figure 7a**. This, in conjunction with utilization of a glass frit rather than an anion exchange membrane, leads to increased coulombic efficiency (average value of 92% in MeCN). Following completion of analysis of the cycling behaviour of $[Ti_2V_4O_5(OMe)_{14}]$ in MeCN, we next performed similar experiments in the composite solvent mixtures. These studies targeted an improved correlation of electron transfer kinetics and battery performance. A complete analysis of 1:1 MeCN:PC, 80:20 MeCN:PC and pure PC battery data is provided in the supporting information file (Figures S47 – S49). Capacities were normalized to the theoretical capacity. Values for subsequent cycles and other solvent systems are described as percentages of this value (**Figure 8**). The initial capacities differ between solvent mixtures when the same cut-off voltage is maintained. Furthermore, the amount of charge passed to reach this cut-off voltage decreases to a differing extent, with the largest loss of normalized capacity occurring in pure PC. No obvious correlations can be made between cycling performance and electrokinetic data collected via cyclic voltammetry. However, across the differing solvent systems changes in active material degradation was observed. Post cycling analysis of the negative electrolyte through cyclic voltammetry (Figure S46 – S49) revealed a decrease in the current response of the $\mathbf{1^+/0}$ redox couple in all solvent systems. The extent of degradation correlates to capacity loss in all experiments (**Figure 8b**); the percentage decrease in current response, indicative of a decrease in concentration of active species over the course of cycling experiments, corresponds to the percentage capacity loss calculated by comparing the charging capacity for cycle 20 to the charging capacity for cycle 1 for each individual solvent system, maintaining the same cut-off voltage throughout. Based on charge/discharge experiments, the chemical stability of the cluster would need to be improved across all solvent systems to further assess the implications of improved electron transfer kinetics in flow-cell applications.

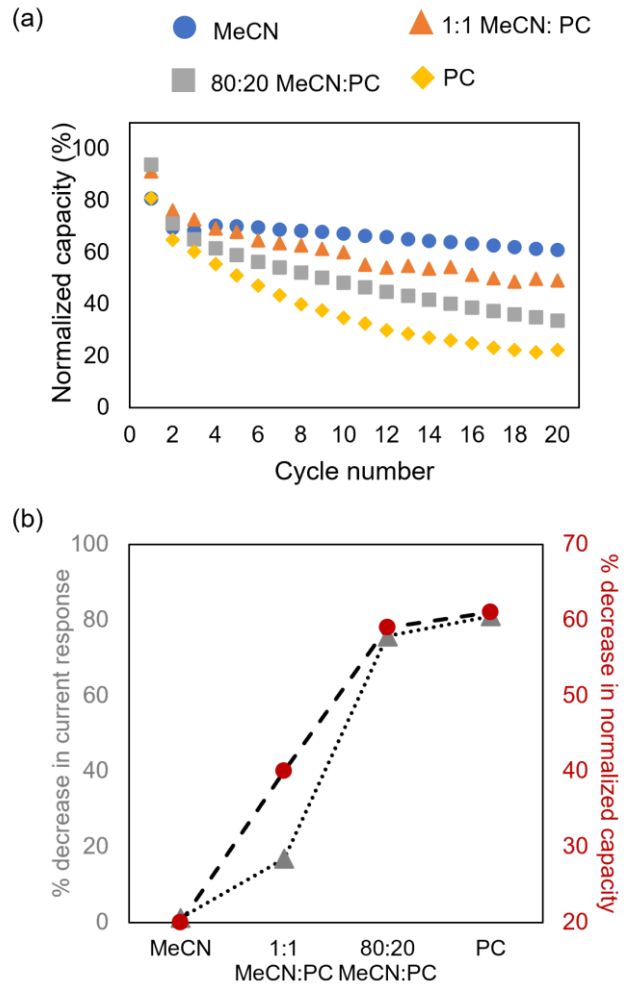

Figure 8. Comparison of (a) capacity normalized to the theoretical capacity of 5 mM active species, and (b) Percentage decrease in current response of the **1^+/0** redox couple and normalized capacity across MeCN – PC mixtures.

Conclusions

In this work, we have employed electrochemical analysis to understand diffusion and electron transfer kinetics of a titanium-substituted POV-alkoxide in various organic solvents. We found that the kinetics of $[Ti_2V_4O_5(OMe)_{14}]$ in each of the five solvents (MeCN, PC, DCM, DMSO and DMF) were fast ($\geq 10^{-2}$ cm/s) for both oxidation and reduction of the cluster. Rapid heterogeneous electron transfer kinetics of charge carriers is desirable, as it gives rise to smaller overpotentials and higher efficiencies for operating RFB devices. Notably, these electron transfer rate constants are an order of magnitude faster than leading contenders for commercially viable charge carriers for non-aqueous RFB technolgoies.[41, 49, 52, 76] Our investigations into factors that influence electron transfer kinetics of the metal oxide assembly have also revealed an inverse relationship between the acceptor number of the solvent and k_0 for the one electron reduction process, which suggests that the acidity of the solvent stabilizes the reduced species. This decreases the free energy barrier between the neutral cluster and the transition state, thereby increasing the rate of electron transfer. No similar solvent property could be correlated to the one electron oxidation process, suggesting a disparate mechanism of electron transfer which could have implications in future battery design.

Additional studies probing the electrokinetic behaviour of the titanium-substituted POV-alkoxide clusters in mixed solvent systems highlight the influence of intermolecular interactions on heterogeneous electron transfer. As compared to previous studies involving $V(acac)_3$ as the charge carrier, $[Ti_2V_4O_5(OMe)_{14}]$ exhibits electron transfer kinetics that are at least an order of magnitude faster for both oxidation and reduction events in mixed solvent systems. For instance, Almheiri and coworkers' study on $V(acac)_3$ in binary and ternary solvent mixtures reported improvements in reaction rates for one or both $V(acac)_3$ disproportionation reactions when small quantities of DMF and 1,3-dioxalane were added to MeCN.[36] This result is consistent with our own observations of improved electron transfer rate constants when 20% (v/v) PC is added to MeCN. Finally, the present study highlights how active material decomposition can vary as a function of solvent composition and that solvent mixtures that yield faster k_0 values can also yield faster rates of decomposition.

The incorporation of charge/discharge data in this work renders our study distinct from prior reports investigating charge carrier electron transfer kinetics with relevance to the development of non-aqueous RFB technologies. While two prior studies have probed ideal solvent combinations for the of enhancing charge carrier solubility and electron transfer kinetics for $V(acac)_3$, neither report probed the influence of these factors on battery performance. We note that while improved electron transfer kinetics were observed in solvent mixtures, more rapid decomposition of the charge carrier was noted in the 80:20 mixture of MeCN and PC.

Overall, this work demonstrates that a thorough understanding of atomistic interactions between solvent and charge carrier can aid in improving the electron transfer kinetics, while maintaining charge carrier stability and appreciable solubility. We conclude that both transport phenomena and heterogeneous rates of electron transfer depend critically on solvent characteristics, and it is possible to tune these properties by carefully selecting the solvent(s) for the electrolyte system. The subtle details associated with such processes need to be understood well to design molecules that serve as excellent charge carriers for applications in non-aqueous RFBs.

Author Contributions

M. D., J. R. M., and E. M. M. conceived and planned the experiments. M. D. and M. C. performed all synthetic and electrochemical experiments and interpreted results. T.R.C. offered invaluable feedback on charge/discharge experiments that lead to publishable findings. All authors contributed in the writing of the manuscript.

Conflicts of interest

J.R.M. is currently an advisory board member and may in the future gain equity interest in a company that develops technologies for redox flow batteries.

Acknowledgements

The authors would like to thank Dr. William W. Brennessel for helpful discussions. The authors would also like to thank Pamela Agredo for guidance during viscosity measurements. This research was funded by the National Science Foundation, Division of Chemical, Bioengineering, Environmental, and Transport Systems Program (Award 2015749).

Notes and references

1. Dunn, B.; Kamath, H.; Tarascon, J. M. Electrical Energy Storage for the Grid: A Battery of Choices. *Science* **2011**, *334*, 928-935. DOI: 10.1126/science.1212741
2. Soloveichik, G. L. Flow Batteries: Current Status and Trends. *Chemical Reviews* **2015**, *115*, 11533-11558. DOI: 10.1021/cr500720t
3. Huang, Q. Z.; Wang, Q. Next-Generation, High-Energy-Density Redox Flow Batteries. *Chempluschem* **2015**, *80*, 312-+. DOI: 10.1002/cplu.201402099
4. Nguyen, T.; Savinell, R. F. Flow Batteries. *Electrochemical Society Interface* **2010**, *19*, 54-56. DOI: 10.1149/2.F06103if
5. de Leon, C. P.; Frias-Ferrer, A.; Gonzalez-Garcia, J.; Szanto, D. A.; Walsh, F. C. Redox flow cells for energy conversion. *Journal of Power Sources* **2006**, *160*, 716-732. DOI: 10.1016/j.jpowsour.2006.02.095
6. Ibrahim, O. A.; Kjeang, E. Leveraging co-laminar flow cells for non-aqueous electrochemical systems. *Journal of Power Sources* **2018**, *402*, 7-14. DOI: 10.1016/j.jpowsour.2018.09.013
7. Burgess, M.; Hernandez-Burgose, K.; Schuh, J. K.; Davila, J.; Montoto, E. C.; Ewoldt, R. H.; Rodriguez-Lopez, J. Modulation of the Electrochemical Reactivity of Solubilized Redox Active Polymers via Polyelectrolyte Dynamics. *Journal of the American Chemical Society* **2018**, *140*, 2093-2104. DOI: 10.1021/jacs.7b08353
8. Li, M.; Odom, S. A.; Pancoast, A. R.; Robertson, L. A.; Vaid, T. P.; Agarwal, G.; Doan, H. A.; Wang, Y. L.; Suduwella, T. M.; Bheemireddy, S. R.; Ewoldt, R. H.; Assary, R. S.; Zhang, L.; Sigman, M. S.; Minteer, S. D. Experimental Protocols for Studying Organic Non-aqueous Redox Flow Batteries. *Acs Energy Letters* **2021**, *6*, 3932-3943. DOI: 10.1021/acsenergylett.1c01675
9. Zhang, J. L.; Corman, R. E.; Schuh, J. K.; Ewoldt, R. H.; Shkrob, I. A.; Zhang, L. Solution Properties and Practical Limits of Concentrated Electrolytes for Nonaqueous Redox Flow Batteries. *Journal of Physical Chemistry C* **2018**, *122*, 8159-8172. DOI: 10.1021/acs.jpcc.8b02009
10. Zhao, P.; Zhang, H. M.; Zhou, H. T.; Chen, J.; Gao, S. J.; Yi, B. L. Characteristics and performance of 10 kW class all-vanadium redox-flow battery stack. *Journal of Power Sources* **2006**, *162*, 1416-1420. DOI: 10.1016/j.jpowsour.2006.08.016
11. Milshtein, J. D.; Tenny, K. M.; Barton, J. L.; Drake, J.; Darling, R. M.; Brushett, F. R. Quantifying Mass Transfer Rates in Redox Flow Batteries. *Journal of the Electrochemical Society* **2017**, *164*, E3265-E3275. DOI: 10.1149/2.0201711jes
12. Aaron, D. S.; Liu, Q.; Tang, Z.; Grim, G. M.; Papandrew, A. B.; Turhan, A.; Zawodzinski, T. A.; Mench, M. M. Dramatic performance gains in vanadium redox flow batteries through modified cell architecture. *Journal of Power Sources* **2012**, *206*, 450-453. DOI: 10.1016/j.jpowsour.2011.12.026
13. Sawant, T. V.; Yim, C. S.; Henry, T. J.; Miller, D. M.; McKone, J. R. Harnessing Interfacial Electron Transfer in Redox Flow Batteries. *Joule* **2021**, *5*, 360-378. DOI: 10.1016/j.joule.2020.11.022
14. Matsuda, Y.; Tanaka, K.; Okada, M.; Takasu, Y.; Morita, M.; Matsumurainoue, T. A RECHARGEABLE REDOX BATTERY UTILIZING RUTHENIUM COMPLEXES WITH NON-AQUEOUS ORGANIC ELECTROLYTE. *Journal of Applied Electrochemistry* **1988**, *18*, 909-914. DOI: 10.1007/bf01016050
15. Chakrabarti, M. H.; Dryfe, R. A. W.; Roberts, E. P. L. Evaluation of electrolytes for redox flow battery applications. *Electrochimica Acta* **2007**, *52*, 2189-2195. DOI: 10.1016/j.electacta.2006.08.052
16. Sleightholme, A. E. S.; Shinkle, A. A.; Liu, Q. H.; Li, Y. D.; Monroe, C. W.; Thompson, L. T. Non-aqueous manganese acetylacetonate electrolyte for redox flow batteries. *Journal of Power Sources* **2011**, *196*, 5742-5745. DOI: 10.1016/j.jpowsour.2011.02.020
17. Zhang, D. P.; Lan, H. J.; Li, Y. D. The application of a non-aqueous bis(acetylacetone)ethylenediamine cobalt electrolyte in redox flow battery. *Journal of Power Sources* **2012**, *217*, 199-203. DOI: 10.1016/j.jpowsour.2012.06.038
18. Kim, J. H.; Kim, K. J.; Park, M. S.; Lee, N. J.; Hwang, U.; Kim, H.; Kim, Y. J. Development of metal-based electrodes for non-aqueous redox flow batteries. *Electrochemistry Communications* **2011**, *13*, 997-1000. DOI: 10.1016/j.elecom.2011.06.022
19. Barton, J. L.; Wixtrom, A. I.; Kowalski, J. A.; Qian, E. A.; Jung, D.; Brushett, F. R.; Spokoyny, A. M. Perfunctionalized Dodecaborate Clusters as Stable Metal-Free Active Materials for Charge Storage. *Acs Applied Energy Materials* **2019**, *2*, 4907-4913. DOI: 10.1021/acsaem.9b00610
20. Balzer, D.; Kassal, I. Even a little delocalization produces large kinetic enhancements of charge-separation efficiency in organic photovoltaics. *Science Advances* **2022**, *8*. DOI: 10.1126/sciadv.abl9692
21. Hogue, R. W.; Toghill, K. E. Metal coordination complexes in nonaqueous redox flow batteries. *Current Opinion in Electrochemistry* **2019**, *18*, 37-45. DOI: 10.1016/j.coelec.2019.08.006
22. Chen, J.-J. J.; Barteau, M. A. Electrochemical Properties of Keggin-Structure Polyoxometalates in Acetonitrile: Effects of Countercation, Heteroatom, and Framework Metal Exchange. *Industrial & Engineering Chemistry Research* **2016**, *55*, 9857-9864. DOI: 10.1021/acs.iecr.6b02316
23. VanGelder, L. E.; Schreiber, E.; Matson, E. M. Physicochemical implications of alkoxide "mixing" in polyoxovanadium clusters for nonaqueous energy storage. *Journal of Materials Chemistry A* **2019**, *7*, 4893-4902. DOI: 10.1039/c8ta12306c

24. Vangelder, L. E.; Kosswattaarachchi, M., A.; Forrestel, P. L.; Cook, T. R.; Matson, E. M. Polyoxovanadate-alkoxide clusters as multi-electron charge carriers for symmetric non-aqueous redox flow batteries. *Chemical Science* **2018**, *9*, 1692-1699. DOI: 10.1039/c7sc05295b
25. Vangelder, L. E.; Forrestel, P. L.; Brennessel, W. W.; Matson, E. M. Site-selectivity in the halogenation of titanium-functionalized polyoxovanadate–alkoxide clusters. *Chemical Communications* **2018**, *54*, 6839-6842. DOI: 10.1039/c8cc01517a
26. Chen, J. J. J.; Barteau, M. A. Molybdenum polyoxometalates as active species for energy storage in non-aqueous media. *Journal of Energy Storage* **2017**, *13*, 255-261. DOI: 10.1016/j.est.2017.07.017
27. Cao, Y.; Chen, J. J. J.; Barteau, M. A. Systematic approaches to improving the performance of polyoxometalates in non-aqueous redox flow batteries. *Journal of Energy Chemistry* **2020**, *50*, 115-124. DOI: 10.1016/j.jechem.2020.03.009
28. Amin, S.; Cameron, J. M.; Watts, J. A.; Walsh, D. A.; Sans, V.; Newton, G. N. Effects of chain length on the size, stability, and electronic structure of redox-active organic-inorganic hybrid polyoxometalate micelles. *Molecular Systems Design & Engineering* **2019**, *4*, 995-999. DOI: 10.1039/c9me00060g
29. Cameron, J. M.; Holc, C.; Kibler, A. J.; Peake, C. L.; Walsh, D. A.; Newton, G. N.; Johnson, L. R. Molecular redox species for next-generation batteries. *Chemical Society Reviews* **2021**, *50*, 5863-5883. DOI: 10.1039/d0cs01507e
30. Peake, C. L.; Kibler, A. J.; Newton, G. N.; Walsh, D. A. Organic-Inorganic Hybrid Polyoxotungstates As Configurable Charge Carriers for High Energy Redox Flow Batteries. *Acs Applied Energy Materials* **2021**, *4*, 8765-8773. DOI: 10.1021/acsaem.1c00800
31. VanGelder, L. E.; Petel, B. E.; Nachtigall, O.; Martinez, G.; Brennessel, W. W.; Matson, E. M. Organic Functionalization of Polyoxovanadate-Alkoxide Clusters: Improving the Solubility of Multimetallic Charge Carriers for Nonaqueous Redox Flow Batteries. *Chemsuschem* **2018**, *11*, 4139-4149. DOI: 10.1002/cssc.201802029
32. VanGelder, L. E.; Brennessel, W. W.; Matson, E. M. Tuning the redox profiles of polyoxovanadate-alkoxide clusters via heterometal installation: toward designer redox Reagents. *Dalton Transactions* **2018**, *47*, 3698-3704. DOI: 10.1039/c7dt04455k
33. Vangelder, L. E.; Matson, M., Ellen Heterometal functionalization yields improved energy density for charge carriers in nonaqueous redox flow batteries. *Journal of Materials Chemistry A* **2018**, *6*, 13874-13882. DOI: 10.1039/c8ta03312a
34. Wang, X.; Xing, X. Q.; Huo, Y. J.; Zhao, Y. C.; Li, Y. D. A systematic study of the co-solvent effect for an all-organic redox flow battery. *Rsc Advances* **2018**, *8*, 24422-24427. DOI: 10.1039/c8ra02513d
35. Herr, T.; Fischer, P.; Tubke, J.; Pinkwart, K.; Elsner, P. Increasing the energy density of the non-aqueous vanadium redox flow battery with the acetonitrile-1,3-dioxolane-dimethyl sulfoxide solvent mixture. *Journal of Power Sources* **2014**, *265*, 317-324. DOI: 10.1016/j.jpowsour.2014.04.141
36. Bamgbopa, M. O.; Pour, N.; Shao-Horn, Y.; Almheiri, S. Systematic selection of solvent mixtures for non-aqueous redox flow batteries - vanadium acetylacetonate as a model system. *Electrochimica Acta* **2017**, *223*, 115-123. DOI: 10.1016/j.electacta.2016.12.014
37. Wang, H.; Sayed, S. Y.; Luber, E. J.; Olsen, B. C.; Shirurkar, S. M.; Venkatakrishnan, S.; Tefashe, U. M.; Farquhar, A. K.; Smotkin, E. S.; McCreery, R. L.; Buriak, J. M. Redox Flow Batteries: How to Determine Electrochemical Kinetic Parameters. *Acs Nano* **2020**, *14*, 2575-2584. DOI: 10.1021/acsnano.0c01281
38. Wipf, D. O.; Kristensen, E. W.; Deakin, M. R.; Wightman, R. M. FAST-SCAN CYCLIC VOLTAMMETRY AS A METHOD TO MEASURE RAPID, HETEROGENEOUS ELECTRON-TRANSFER KINETICS. *Analytical Chemistry* **1988**, *60*, 306-310. DOI: 10.1021/ac00155a006
39. Myland, J. C.; Oldham, K. B. Uncompensated resistance. 1. The effect of cell geometry. *Analytical Chemistry* **2000**, *72*, 3972-3980. DOI: 10.1021/ac0001535
40. Goulet, M. A.; Aziz, M. J. Flow Battery Molecular Reactant Stability Determined by Symmetric Cell Cycling Methods. *Journal of the Electrochemical Society* **2018**, *165*, A1466-A1477. DOI: 10.1149/2.0891807jes
41. Herr, T.; Noack, J.; Fischer, P.; Tubke, J. 1,3-Dioxolane, tetrahydrofuran, acetylacetone and dimethyl sulfoxide as solvents for non-aqueous vanadium acetylacetonate redox-flow-batteries. *Electrochimica Acta* **2013**, *113*, 127-133. DOI: 10.1016/j.electacta.2013.09.055
42. Wohlfarth, C. *Static Dielectric Constants of Pure Liquids and Binary Liquid Mixtures*. Springer-Verlag, Berlin, Heidelberg: New York, 1991; Vol. 6.
43. Viswanath, D. S.; Natarajan, G. *Data book on the viscosity of liquids*. New York : Hemisphere Pub. Corp., ©1989.: 1989.
44. Marcus, Y. THE PROPERTIES OF ORGANIC LIQUIDS THAT ARE RELEVANT TO THEIR USE AS SOLVATING SOLVENTS. *Chemical Society Reviews* **1993**, *22*, 409-416. DOI: 10.1039/cs9932200409
45. Reichardt, C. EMPIRICAL PARAMETERS OF SOLVENT POLARITY AS LINEAR FREE-ENERGY RELATIONSHIPS. *Angewandte Chemie-International Edition in English* **1979**, *18*, 98-110. DOI: 10.1002/anie.197900981
46. Cabrera, P. J.; Yang, X. Y.; Suttil, J. A.; Brooner, R. E. M.; Thompson, L. T.; Sanford, M. S. Evaluation of Tris-Bipyridine Chromium Complexes for Flow Battery Applications: Impact of Bipyridine Ligand Structure on Solubility and Electrochemistry. *Inorganic Chemistry* **2015**, *54*, 10214-10223. DOI: 10.1021/acs.inorgchem.5b01328
47. Yang, B.; Hoober-Burkhardt, L.; Wang, F.; Prakash, G. K. S.; Narayanan, S. R. An Inexpensive Aqueous Flow Battery for Large-Scale Electrical Energy Storage Based on Water-Soluble Organic Redox Couples. *Journal of the Electrochemical Society* **2014**, *161*, A1371-A1380. DOI: 10.1149/2.1001409jes
48. Liu, Q. H.; Sleightholme, A. E. S.; Shinkle, A. A.; Li, Y. D.; Thompson, L. T. Non-aqueous vanadium acetylacetonate electrolyte for redox flow batteries. *Electrochemistry Communications* **2009**, *11*, 2312-2315. DOI: 10.1016/j.elecom.2009.10.006
49. Shinkle, A. A.; Sleightholme, A. E. S.; Thompson, L. T.; Monroe, C. W. Electrode kinetics in non-aqueous vanadium acetylacetonate redox flow batteries. *Journal of Applied Electrochemistry* **2011**, *41*, 1191-1199. DOI: 10.1007/s10800-011-0314-z

50. Ding, Y.; Zhao, Y.; Li, Y. T.; Goodenough, J. B.; Yu, G. H. A high-performance all-metallocene-based, non-aqueous redox flow battery. *Energy & Environmental Science* **2017**, *10*, 491-497. DOI: 10.1039/c6ee02057g
51. Pan, F.; Wang, Q. Redox Species of Redox Flow Batteries: A Review. *Molecules* **2015**, *20*, 20499-20517. DOI: 10.3390/molecules201119711
52. Hendriks, K. H.; Robinson, S. G.; Braten, M. N.; Sevov, C. S.; Helms, B. A.; Sigman, M. S.; Minteer, S. D.; Sanford, M. S. High-Performance Oligomeric Catholytes for Effective Macromolecular Separation in Nonaqueous Redox Flow Batteries. *Acs Central Science* **2018**, *4*, 189-196. DOI: 10.1021/acscentsci.7b00544
53. Jones, A. E.; Ejigu, A.; Wang, B.; Adams, R. W.; Bissett, M. A.; Dryfe, R. A. W. Quinone voltammetry for redox-flow battery applications. *Journal of Electroanalytical Chemistry* **2022**, *920*, 116572. DOI: https://doi.org/10.1016/j.jelechem.2022.116572
54. Desiraju, G. R.; Paul, I. C.; Curtin, D. Y. CONVERSION IN SOLID-STATE OF YELLOW TO RED FORM OF 2-(4'-METHOXYPHENYL)-1,4-BENZOQUINONE - X-RAY CRYSTAL-STRUCTURES AND ANISOTROPY OF REARRANGEMENT. *Journal of the American Chemical Society* **1977**, *99*, 1594-1601. DOI: 10.1021/ja00447a051
55. Molcanov, K.; Juric, M.; Kojic-Prodic, B. Stacking of metal chelating rings with pi-systems in mononuclear complexes of copper(II) with 3,6-dichloro-2,5-dihydroxy-1,4-benzoquinone (chloranilic acid) and 2,2 '-bipyridine ligands. *Dalton Transactions* **2013**, *42*, 15756-15765. DOI: 10.1039/c3dt51734a
56. Fawcett, W. R.; Foss, C. A. THE ANALYSIS OF SOLVENT EFFECTS ON THE KINETICS OF SIMPLE HETEROGENEOUS ELECTRON-TRANSFER REACTIONS. *Journal of Electroanalytical Chemistry* **1988**, *252*, 221-229. DOI: 10.1016/0022-0728(88)85085-x
57. Marcus, R. A. ON THEORY OF ELECTRON-TRANSFER REACTIONS .6. UNIFIED TREATMENT FOR HOMOGENEOUS AND ELECTRODE REACTIONS. *Journal of Chemical Physics* **1965**, *43*, 679-&. DOI: 10.1063/1.1696792
58. Sumi, H.; Marcus, R. A. Dynamical effects in electron transfer reactions. *The Journal of Chemical Physics* **1986**, *84*, 4894-4914. DOI: 10.1063/1.449978
59. Nicholson, R. S. THEORY AND APPLICATION OF CYCLIC VOLTAMMETRY FOR MEASUREMENT OF ELECTRODE REACTION KINETICS. *Analytical Chemistry* **1965**, *37*, 1351-+. DOI: 10.1021/ac60230a016
60. Sawant, T. V.; McKone, J. R. Flow Battery Electroanalysis. 2. Influence of Surface Pretreatment on Fe(III/II) Redox Chemistry at Carbon Electrodes. *Journal of Physical Chemistry C* **2019**, *123*, 144-152. DOI: 10.1021/acs.jpcc.8b09607
61. Gutmann, V. Solvent effects on the reactivities of organometallic compounds. *Coordination Chemistry Reviews* **1976**, *18*, 225-255. DOI: 10.1016/S0010-8545(00)82045-7
62. Kaneko, H.; Sekine, K.; Takamura, T. Power capability improvement of LiBOB/PC electrolyte for Li-ion batteries. *Journal of Power Sources* **2005**, *146*, 142-145. DOI: 10.1016/j.jpowsour.2005.03.115
63. Wagner, R.; Brox, S.; Kasnatscheew, J.; Gallus, D. R.; Amereller, M.; Celdc-Laskovic, I.; Winter, M. Vinyl sulfones as SEI-forming additives in propylene carbonate based electrolytes for lithium-ion batteries. *Electrochemistry Communications* **2014**, *40*, 80-83. DOI: 10.1016/j.elecom.2014.01.004
64. Wang, B.; Zhang, H. P.; Yang, L. C.; Qu, Q. T.; Wu, Y. P.; Gan, C. L.; Zhou, D. L. Improving electrochemical performance of graphitic carbon in PC-based electrolytes by using N-vinyl-2-pyrrolidone as an additive. *Electrochemistry Communications* **2008**, *10*, 1571-1574. DOI: 10.1016/j.elecom.2008.08.018
65. Xing, L. D.; Wang, C. Y.; Li, W. S.; Xu, M. Q.; Meng, X. L.; Zhao, S. F. Theoretical Insight into Oxidative Decomposition of Propylene Carbonate in the Lithium Ion Battery. *Journal of Physical Chemistry B* **2009**, *113*, 5181-5187. DOI: 10.1021/jp810279h
66. Yun, J. J.; Zhang, L.; Qu, Q. T.; Liu, H. M.; Zhang, X. L.; Shen, M.; Zheng, H. H. A Binary Cyclic Carbonates-Based Electrolyte Containing Propylene Carbonate and Trifluoropropylene Carbonate for 5 V Lithium-Ion Batteries. *Electrochimica Acta* **2015**, *167*, 151-159. DOI: 10.1016/j.electacta.2015.03.159
67. Su, C. C.; He, M. N.; Amine, R.; Chen, Z. H.; Sahore, R.; Rago, N. D.; Amine, K. Cyclic carbonate for highly stable cycling of high voltage lithium metal batteries. *Energy Storage Materials* **2019**, *17*, 284-292. DOI: 10.1016/j.ensm.2018.11.003
68. Oates, W. A. IDEAL SOLUTIONS. *Journal of Chemical Education* **1969**, *46*, 501-&. DOI: 10.1021/ed046p501
69. Afanas'ev, V. N.; Chekunova, M. D.; Tyunina, E. Y. Effect of ultrasound on transport properties of nonaqueous solutions of lithium hexafluoroarsenate. *Russian Journal of Physical Chemistry* **2006**, *80*, 1929-1933. DOI: 10.1134/s0036024406120119
70. Jouyban, A.; Maljaei, S. H.; Soltanpour, S.; Fakhree, M. A. A. Prediction of viscosity of binary solvent mixtures at various temperatures. *Journal of Molecular Liquids* **2011**, *162*, 50-68. DOI: 10.1016/j.molliq.2011.06.002
71. Flanagan, K. B.; Hoover, K. R.; Garza, O.; Hizon, A.; Soto, T.; Villegas, N.; Acree, W. E.; Abraham, M. H. Mathematical correlation of 1-chloroanthraquinone solubilities in organic solvents with the Abraham solvation parameter model. *Physics and Chemistry of Liquids* **2006**, *44*, 377-386. DOI: 10.1080/00319100600805448
72. Braun, R. J.; Parrott, E. L. INFLUENCE OF VISCOSITY AND SOLUBILIZATION ON DISSOLUTION RATE. *Journal of Pharmaceutical Sciences* **1972**, *61*, 175-&. DOI: 10.1002/jps.2600610206
73. Marcus, R. A. Electron transfer reactions in chemistry - Theory and experiment. *Journal of Electroanalytical Chemistry* **1997**, *438*, 251-259. DOI: 10.1016/s0022-0728(97)00091-0
74. Sharma, K.; Sankarasubramanian, S.; Parrondo, J.; Ramani, V. Electrochemical implications of modulating the solvation shell around redox active organic species in aqueous organic redox flow batteries. *Proceedings of the National Academy of Sciences of the United States of America* **2021**, *118*. DOI: 10.1073/pnas.2105889118
75. Cabrera, P. J.; Yang, X. Y.; Sutti, J. A.; Hawthorne, K. L.; Brooner, R. E. M.; Sanford, M. S.; Thompson, L. T. Complexes Containing Redox Noninnocent Ligands for Symmetric, Multielectron Transfer Nonaqueous Redox Flow Batteries. *Journal of Physical Chemistry C* **2015**, *119*, 15882-15889. DOI: 10.1021/acs.jpcc.5b03582

76. Morita, M.; Tanaka, Y.; Tanaka, K.; Matsuda, Y.; Matsumurainoue, T. ELECTROCHEMICAL OXIDATION OF RUTHENIUM AND IRON COMPLEXES AT ROTATING-DISK ELECTRODE IN ACETONITRILE SOLUTION. *Bulletin of the Chemical Society of Japan* **1988**, *61*, 2711-2714. DOI: 10.1246/bcsj.61.2711.